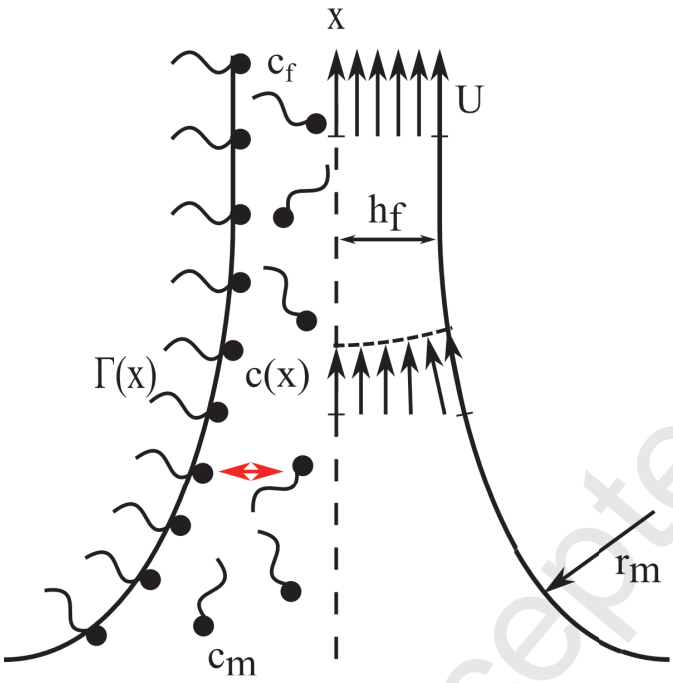

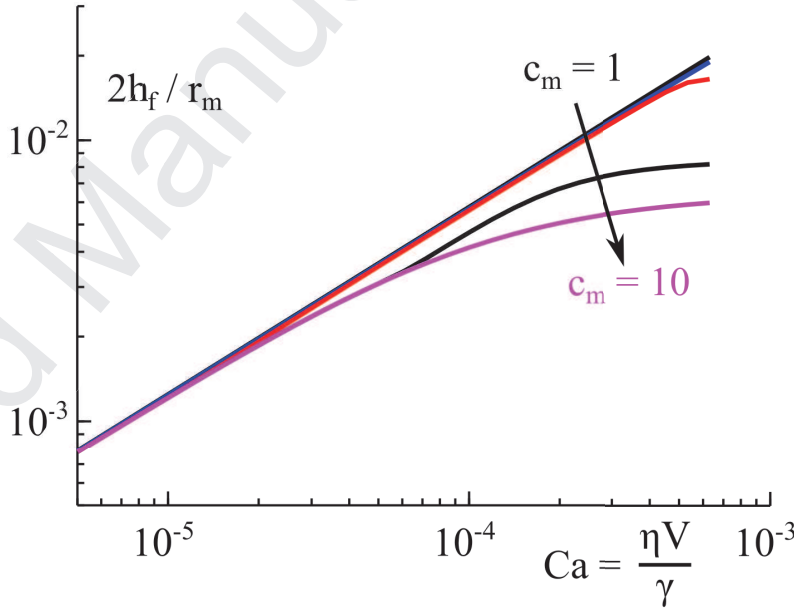

Highlight

- Deviation from the Frankel's law predicting the soap film thickness is computed.
- The film thickness varies non-monotonically with the surfactant bulk concentration.
- The elastic interface behavior is recovered at small solubility.
- The predictions are compatible with available experimental data.

Generation of soap films with instantaneously adsorbed surfactants: concentration-dependent film thinning

J. Seiwert[a], I. Cantat[a,*]

[a] *Institut de Physique de Rennes, UMR 6251 CNRS/Université de Rennes 1, Rennes, France.*

Abstract

In this theoretical work, we predict the steady state thickness of soap films pulled from a bath of surfactants. Assuming simplified thermodynamical properties for the surfactants, we compute the interfacial stresses by taking explicitly into account surfactant convection along the film. We make no assumption on interfacial rheology: the rigidification of the interfaces results entirely from confinement and depletion effects. Two main approximations are used: the concentration of surfactants is supposed homogeneous within the thickness of the film, and at equilibrium with the adsorbed layer. With these hypothesis, we show that the thickness of the film follows Frankel's law at low capillary numbers, and that deviations occur at higher pulling velocities. We study the dependence of the film thickness with the characteristics of the surfactant used and especially with its initial concentration, and we show that our predictions are compatible with available data by Saulnier and coworkers.

1. Introduction

The generation of soap films when extracted from a bath at a constant velocity is one of the staple problems featuring hydrodynamics in the presence of surfactants. The great and constant interest in this seemingly simple set up has several origins: it appears in numerous industrial processes, and it features

*Corresponding author
Email address: isabelle.cantat@univ-rennes1.fr +33 2 23 23 56 28 (I. Cantat)

the same key ingredients as the central mechanisms for foam evolution and rheology, namely the coupling between hydrodynamics and surfactant dynamics. By extending the work of Landau, Levich [1] and Derjaguin [2], Frankel [3] has first predicted the steady state thickness of the film and its power law dependency with the capillary number $\mathrm{Ca} = \eta U/\gamma$, with U the pulling velocity, η the solution viscosity and γ its surface tension. Numerous experimental studies have confirmed the great accuracy of this theory, over a large range of capillary numbers and for a large sample of surfactant solutions [4, 5, 6].

However, at large enough capillary numbers, several surfactant solutions exhibit a clear deviation from Frankel's law [7, 8, 9]: the measured film thickness is lower than predicted by Frankel, and exhibits a maximum at a given capillary number. In [7, 8, 10, 9], these observations are explained by a finite elasticity of the interface. Scaling analysis shows that a deviation from the Frankel's law, which assumes incompressible interfaces, is expected for capillary numbers larger than $(E/\gamma)^{3/2}$, with $E = \partial\gamma/\partial(\ln(A))$ the elasticity of the interface. Depending on the type of surfactant used, this may or may not be in the range of capillary numbers accessible to experiments, which explains why only some solutions exhibit the aforementioned deviation. The main shortcoming of this approach is related to the fact the underlying physical mechanisms at the origin of the elasticity E are most often not explicited.

For insoluble surfactants with negligible surface diffusion, or when the exchange of surfactant between the interface and the bulk is slow enough that it can be excluded from the process, this elasticity arises directly from the variation of surface tension with the surface excess Γ. Indeed, in that case mass conservation of surfactants implies that $A\Gamma$ be constant so $d\ln(\Gamma) = -d\ln(A)$ and thus $E = -\partial\gamma/\partial\ln(\Gamma)$. This elasticity is known as the Marangoni elasticity E_M [11].

However, for soluble surfactants, exchange with the bulk phase modifies the mass balance equation and the interface elasticity becomes an effective quantity which potentially depends on the complicated interplay between surfactant dynamics and hydrodynamics, through advection, diffusion and adsorption pro-

cesses. As a general picture, fast adsorbing surfactants may repopulate instantly any interface that is stretched, and should not lead to any interfacial gradients and Marangoni stresses: the effective elasticity or viscosity associated with exchanges with the bulk should vanish for such surfactants. The film systems that we consider here, however, have a very peculiar aspect ratio, as their thickness is generally several orders of magnitude smaller than their extent.

In such confined films, the physical origin of interfacial stresses, and thus of the effective interfacial elasticity, is generally assumed to lie in surfactant depletion within the film [12, 11, 13]. As interfaces stretch, surfactant molecules within the volume of the film are adsorbed, thereby lowering locally their concentration, increasing locally surface tension and generating Marangoni stresses. This depletion effect becomes important if the thickness of the film becomes smaller than the typical length $l_q = \Gamma/c$, where Γ and c are respectively the interface and volume concentration of surfactant [13]. For typical surfactants used in film withdrawal experiments, this length varies between 1 µm and 100 µm, which is comparable or larger than film thicknesses (1 µm to 10 µm).

When the thin film deformation is a pure stretching deformation, a film element constitutes a closed system. The surfactant mass balance, involving interface and bulk contributions, can thus still be used to relate area variations to surface excess variations. This leads to the definition of an effective surface elasticity of the film, namely the Gibbs elasticity E_G [12, 11], that consistently takes into account the depletion effect. In contrast, in more complex dynamical situations, such as film extraction, the velocity of the fluid is not homogeneous across the width of the film, and the local mass balance at the origin of the definition of the Gibbs modulus is not valid anymore. Surfactants are convected along the film and interface stretching at a given place of the film can therefore lead to a surface tension increase at another place of the film. An effective surface elasticity, coupling locally area variation and surface tension, can not be rigorously defined.

We present here a model that rationalizes the depletion effect involved in the film generation process. The model takes surfactants convection explicitly

into account by tracking surfactant concentrations in the volume and at the interface. We consider the case where surfactant adsorption is instantaneous: our model thus predicts the thickness of soap films for a given surfactant solution from its equilibrium isotherm and equation of state. Both the incompressible interface behavior and the elastic interface behavior are recovered, as limiting cases in the parameter space. This model allows a better understanding of surfactant transport phenomena, and, despite its approximations, it does compare favorably with experimental data.

2. Model

The problem that we consider is sketched on figure 1. A film is withdrawn at a constant velocity U from a meniscus acting as a reservoir of surfactant solution (viscosity η, surface tension γ_m). We neglect the effect of gravity, so that the meniscus features, at rest, a constant radius of curvature r_m. We further assume the problem to be bidimensionnal (the film has an infinite width in the z direction, perpendicular to the plane of the sketch), and we focus on steady state: far from the meniscus, the film has a constant thickness $2h_f$.

In typical experiments, h_f is on the order of micrometers, while the meniscus has a millimetric size. This large difference in sizes allows for the classical division of the system in three distinct regions [1]: 1) the flat film at the top, which is translated at a constant velocity U; 2) the static meniscus, a the region of negligible flow where the meniscus is unperturbed and; 3) the dynamical meniscus of length ℓ and of typical thickness h_f bridging the two, where viscous and pressure forces balance.

2.1. Scaling analysis of Frankel's law

In Frankel's theory, the interfaces are incompressible, and they move with the tangent velocity U imposed by the operator. In that case, the viscous force (per unit volume) in the dynamic meniscus scales like $\eta U/h_f^2$. Moreover, the dynamic meniscus connects the flat film, where the pressure is p_0 (the atmospheric pressure), to the static meniscus where the pressure is $p_0 - \gamma/r_m$. The

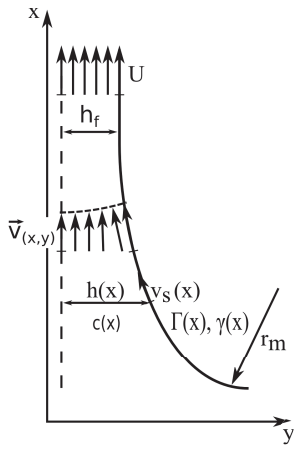

Figure 1: Sketch of the problem: only half of the film is represented, the dashed line represents an axe of symmetry of the problem. The film is extracted at a constant velocity U from a meniscus of constant radius of curvature r_m. We compute its half thickness profile $h(x)$, the interfacial velocity $v_s(x)$ and the concentration of surfactant $c(x)$. Γ and γ are respectively the interfacial concentration of surfactants, and the surface tension.

balance between pressure gradient and viscous forces thus writes:

$$\frac{\eta U}{h_f^2} \sim \frac{\gamma}{r_m \ell}$$

The length ℓ of the dynamic meniscus is determined by imposing that its curvature (of order h_f/ℓ^2) matches that of the static meniscus ($1/r_m$) to ensure the continuity of pressure, so that $\ell \sim \sqrt{r_m h_f}$. The well known prediction for the thickness of the film follows [3]:

$$h_f = 1.34 r_m \mathrm{Ca}^{2/3}$$

with $\mathrm{Ca} = \eta U/\gamma$ the capillary number. A consequence of this scaling is the length of the dynamic meniscus: $\ell \sim r_m \mathrm{Ca}^{1/3}$.

2.2. Marangoni stresses and elastic interfaces

Another prediction deduced from Frankel's model is the stress arising at the interface in order to pull the film out of the reservoir. It does not appear explicitly in the calculation, since the imposed constant velocity U is used as

boundary condition instead. However, it can be computed from the velocity field, since the surface tension gradient must balance, at each position along the interface, the viscous stress in the bulk of the film. This gradient is confined to the dynamical meniscus, and scales like $\eta U/h_f$ [14].

In other words, the surface tension γ_f in the flat film region must be slightly larger than the surface tension γ_m in the static meniscus, in order to balance viscous dissipation and extract the film. Their difference $\Delta\gamma = \gamma_f - \gamma_m$ is [10]

$$\frac{\Delta\gamma}{\gamma} = \frac{\gamma_f - \gamma_m}{\gamma_m} = 3.84\mathrm{Ca}^{2/3} \tag{1}$$

Frankel's theory assumes perfectly incompressible interfaces, where any surface tension difference may be generated with negligible interface deformation. For elastic interfaces, on the other hand, this difference in surface tension $\Delta\gamma$ originates from a relative increase of interface area $\Delta A/A$ which depends on the interface elastic modulus: $\Delta A/A = \Delta\gamma/E \sim \mathrm{Ca}^{2/3}\gamma_m/E$. As pointed out earlier [7, 9, 10], when $\mathrm{Ca} \gtrsim (E/\gamma)^{3/2}$, interfacial deformation becomes non negligible, and deviations from Frankel's law are observed.

The elastic model will appear as a limit, for poorly soluble surfactants, of the more complex model presented below.

2.3. Surfactant transport

Our model for surfactant transport is based on two main approximations:

1. surfactant concentration $c(x)$ is homogeneous in the direction of the film thickness.
2. surfactant adsorption is instantaneous, so that bulk concentration $c(x)$ is always at equilibrium with surface excess $\Gamma(x)$.

Stresses and surface deformations only occur in the dynamical meniscus, so the validity of these approximations needs to be satisfied in this region. Concentration gradients across the thickness of the film decay by diffusion with a typical time $t_D^{\perp} = h_f^2/D \sim r_m^2\mathrm{Ca}^{4/3}/D$, where D is the diffusion coefficient for the surfactant. On the other hand, changes in subsurface concentration

occur on the time scale of the transit in the dynamical meniscus $t_{dyn} = \ell/U \sim r_m \mathrm{Ca}^{1/3}/U = \mathrm{Ca}^{-2/3}\eta r_m/\gamma$.

Approximation 1 is valid as long as $t_D^{\perp} \ll t_{dyn}$, that is $\mathrm{Ca} \ll \mathrm{Ca}_D = \sqrt{\eta D/\gamma r_m}$. With typical aqueous surfactant solutions ($D \approx 10^{-10}$ m^2/s, $\eta \approx 1$ mPa$\cdot$s, $\gamma \approx 30$ mN/m and $r_m = 1$ mm), $\mathrm{Ca}_D \approx 10^{-4}$ is close to the upper limit of the range of capillary numbers tested in experiments ($\mathrm{Ca} = 10^{-6}$–10^{-3}), and approximation 1 is well satisfied at low velocities.

Evaluating approximation 2 requires the typical adsorption time t_{ads} of the surfactant. To estimate it, we assume a linear kinetics adsorption (Henry kinetics), where the flux of adsorbed surfactant molecules is proportional to the bulk concentration, and to the deviation from the equilibrium interfacial concentration: $j = kc\,(1 - \Gamma/\Gamma_{eq})$ [15]. Assuming small deviations of c and Γ around an equilibrium value, the equation for $\Delta\Gamma = \Gamma - \Gamma_{eq}$ becomes, at first order in deviations from equilibrium, $\frac{d\Delta\Gamma}{dt} = -kc_{eq}\frac{\Delta\Gamma}{\Gamma_{eq}}$. The interface thus repopulate on a timescale $t_{ads} = \frac{\Gamma_{eq}}{kc_{eq}} = \frac{l_q}{k}$.

The value of k depends on the surfactant used, and in the simplest cases it may be evaluated as a diffusion speed on a molecular length scale a [13]: $k = D/a$. With $a = 1$ nm and $D = 10^{-10}$ m^2/s, $k \approx 0.1$ m/s. The ratio $l_q = \frac{\Gamma_{eq}}{c_{eq}}$ depends strongly on the concentration, and on the surfactant used. At the critical micellar concentration (cmc), l_q varies for example between 1 µm for Sodium Dodecyl Sulfate, and 1 cm for Triton X-100 [15]. Above the cmc, since Γ remains approximately constant, the above estimations need to be multiplied by a factor c/c_{cmc}, that may be of the order of 10. With these values, t_{ads} varies between $10^{-5} - 10^{-1}$ s. For the fastest surfactants, t_{ads} is always much shorter than t_{dyn} ($10^{-2} - 1$ s), and approximation 2 is well satisfied. For other surfactants, however, this approximation is not correct anymore: the slowest surfactants behave like insoluble surfactants in this problem.

These set of approximations has been used previously to study the static thickness of soap films [16] and the (slow) drainage of Plateau borders [17] in the field of gravity. We showed here that their validity can be extended to our case.

In the following, we will also neglect any diffusion in the direction along the film (both in the volume and at the interface). Indeed, comparing a diffusion time based on ℓ with t_{dyn} shows that longitudinal diffusion is negligible as long as $\mathrm{Ca} \gg (\eta D/\gamma r_m)^{3/4} \approx 10^{-6}$. This is a very well satisfied approximation, since in most experiments other phenomena (such as disjoining pressure, evaporation, etc.) would become dominant at such low capillary numbers.

Lastly, we use the same set of hydrodynamics approximation as Frankel, namely: we assume a gravity free lubrication flow in the dynamical meniscus and match it asymptotically to both the static meniscus and the film.

2.4. Shape of the dynamic meniscus

As we mentioned earlier, we model the dilution of surfactants that generates the necessary Marangoni stresses in the dynamic meniscus. The dilution is driven by interface stretching: correspondingly, interfacial velocity increases along the dynamical meniscus (from the static meniscus to the film). Five variables need to be tracked: the half with $h(x)$ of the film, the bulk and interfacial surfactant concentrations $c(x)$ and $\Gamma(x)$, the surface tension $\gamma(x)$ and the interfacial velocity $v_s(x)$.

The adsorption isotherm and the equation of state relate γ and Γ to c (see section 2.5), so three additional equations are needed to close the problem. These come from the conservation of the volume flux along the film, the balance of stresses at the interface and the conservation of surfactant molecules.

With the usual lubrication assumptions, symmetry around $y = 0$ and an interfacial velocity $v_s(x)$, the x-component of the fluid velocity within the film writes, at dominant order in h_f/ℓ (subscripts are used to denote derivations) :

$$v(x,y) = -\frac{\gamma h_{xxx}}{2\eta}\left(y^2 - h^2\right) + v_s(x) \tag{2}$$

At steady state, the volume flux q (in the half film) must be constant along the film, and may be evaluated in the flat film region where $q = Uh_f$ (with U the imposed velocity), giving the differential equation for h in the dynamic

meniscus:

$$q = Uh_f = \frac{\gamma h_{xxx}}{3\eta} h^3 + v_s h \tag{3}$$

The second equation relates the distribution of γ to the underlying flow by expressing the balance between the bulk viscous stress and Marangoni forces at the interface:

$$\frac{\partial \gamma}{\partial x} = \eta \left.\frac{\partial v}{\partial y}\right|_h = -\gamma h_{xxx} h \tag{4}$$

The last relation that we use expresses the conservation of surfactant molecules. Since we neglect diffusion in the x direction, the flux of surfactants is only due to convection, and it has a bulk and a surface contribution: $q_{surf} = cq + \Gamma v_s$. It must be constant with respect to x at steady state:

$$\frac{\partial}{\partial x}\left(cq + \Gamma v_s\right) = 0 \tag{5}$$

Boundary conditions for h and v_s are specified in the flat film region: for $x \to +\infty$, they must asymptote to constant values h_f, and U. c, γ and Γ must also reach constant values c_f, γ_f and Γ_f. However, in practice the concentration, and thus the value of γ and Γ, is imposed in the static meniscus, which acts as a reservoir for surfactants due to its large size. Thus, the physical boundary condition for those variables is imposed for $x \to -\infty$, where $c = c_m$, $\gamma = \gamma_m$ and $\Gamma = \Gamma_m$.

2.4.1. System of equations

Surfactants are assumed to equilibrate instantaneously between the interface and the bulk (assumption 2), so that the equilibrium equation of state and adsorption isotherm may be used to relate respectively γ to Γ and Γ to c. We discuss the shape of these functions in the next section, but we take them formally into account here by treating γ and Γ as functions of respectively Γ and c only.

Equation 4 is rewritten, using equation 3, as:

$$\frac{\partial \gamma}{\partial \Gamma}\frac{\partial \Gamma}{\partial c} c_x = -3\eta \frac{Uh_f - v_s h}{h^2} \tag{6}$$

Equation 5 is integrated between x and the flat film region, where $\Gamma(x) = \Gamma_f$, $v_s(x) = U$, $c(x) = c_f$, $\gamma(x) = \gamma_f$, $h(x) = h_f$

$$Uh_f(c - c_f) + v_s\Gamma - U\Gamma_f = 0 \tag{7}$$

2.5. Adsorption isotherm and equation of state

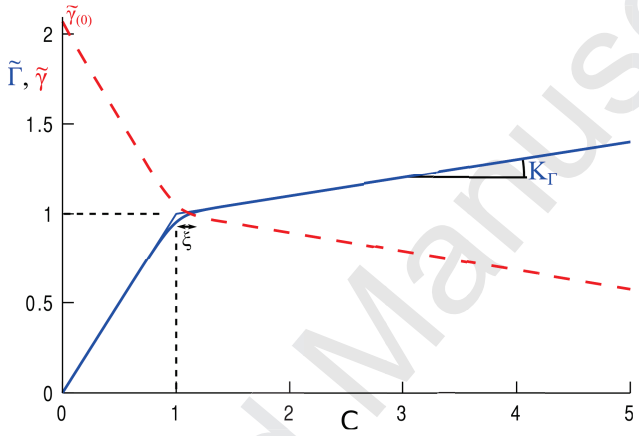

Figure 2: Blue solid line: non dimensional adsorption isotherm $\tilde{\Gamma} = \Gamma/\Gamma_{cmc}$ as a function of $C = c/c_{cmc}$, which is affine far enough below and above the critical micellar concentration ($C = 1$), with slopes equal to 1 and K_Γ. The transition region has a thickness ξ (throughout this study $\xi = 0.15$). Red dashed line: non dimensional surface tension $\tilde{\gamma} = \gamma/\gamma_{cmc}$ as a function of C. The equation of state $\tilde{\gamma}(\tilde{\Gamma})$ is affine on the entire range, its only free parameter is the surface tension of the pure liquid $\tilde{\gamma}(0)$ (throughout this study $\tilde{\gamma}(0) = 72/35 \approx 2.1$).

For the sake of simplicity we use simplified analytical expressions for the adsorption isotherm and the equation of state. Note that it is not necessary for our calculations, and arbitrary functions could be used instead. The adsorption isotherm $\Gamma(c)$ has been chosen as a derivable function satisfying the two following important properties: a rapid increase of Γ from 0 to Γ_{cmc} when c increases from 0 to the cmc, and a saturation of Γ above the cmc. Indeed, we found that the non linearity in the isotherm is crucial for the generation of films (see section 4.4, incidentally, it is the main difference, regarding surfactants dynamics, between our model, and the aforementioned studies on static films [16] and Plateau

border drainage [17]). More precisely, we impose

$$\frac{\Gamma}{\Gamma_{cmc}} = \frac{1+K_\Gamma}{2}\frac{c}{c_{cmc}} + \frac{1-K_\Gamma}{2}\left(1 - \xi \log\left[e^{\frac{c/c_{cmc}-1}{\xi}} + e^{-\frac{c/c_{cmc}-1}{\xi}}\right]\right) \qquad (8)$$

whose graph is plotted on figure 2. The parameter ξ is the size of the transition region at the cmc. It does not affect the result of the model as long as it is small enough.

Below the cmc, the above expression asymptotes to the linear relation $\Gamma/\Gamma_{cmc} = c/c_{cmc}$. Due to the transition region, Γ is close, but slightly below, Γ_{cmc} for $c = c_{cmc}$. Above the transition, the adsorption isotherm reduces to $\Gamma/\Gamma_{cmc} = 1 + K_\Gamma(c/c_{cmc} - 1)$. We chose an affine relation with a very small slope K_Γ above the cmc instead of a strict saturation. A non vanishing value for K_Γ is indeed required for numerical stability. We additionally believe that this parameter K_Γ is a physical parameter, even if difficult to measure. Stubenrauch and collaborators [18] measured for example a decrease of the surface tension of a solution of $C_{12}E_6$ close to 2 mN/m as the concentration goes from $c = c_{cmc}$ to $c = 10\,c_{cmc}$. Even such a small variation of γ above the cmc may not be neglected a priori: as we already stressed, in these films, minute surface tension variations (on the order of 0.01 % to 1%, that is 0.01 to 1 mN/m) have a strong effect.

Finally, we assume an affine relationship between γ and Γ. The equation of state is thus

$$\frac{\gamma}{\gamma_{cmc}} = \frac{\gamma(0)}{\gamma_{cmc}} - \frac{\Gamma}{\Gamma_{cmc}}\left(\frac{\gamma(0)}{\gamma_{cmc}} - 1\right) \qquad (9)$$

with $\gamma(0)$ the surface tension of pure water.

3. Numerics

3.1. Rescaling

We define the dimensionless variables as follows, and separate them by uppercasing, or tilding. h and v_s are rescaled by their value in the flat film: $H = h/h_f$, $V_s = v_s/U$. The concentrations and the surface tension are rescaled by their value at the cmc: $C = c/c_{cmc}$, $\tilde{\Gamma} = \Gamma/\Gamma_{cmc}$, $\tilde{\gamma} = \gamma/\gamma_{cmc}$. Consistently,

the space variable becomes $X = x\mathrm{Ca_c}^{1/3}/h_f$ with $\mathrm{Ca_c} = \eta U/\gamma_{cmc}$. This capillary number Ca is based on the value of surface tension at the cmc. It is slightly different than the capillary number used, for example, to describe experimental studies, based on the surface tension of the solution (at whatever surfactant concentration is used), which we denote by Ca.

Equations 3, 6 and 7 become, with $\tilde{\Gamma}$ and $\tilde{\gamma}$ explicit functions of C given by equations 9 and 8:

$$H_{XXX} = \frac{3}{\tilde{\gamma}} \frac{1 - V_s H}{H^3} \tag{10}$$

$$\frac{\partial \tilde{\gamma}}{\partial \tilde{\Gamma}} \frac{\partial \tilde{\Gamma}}{\partial C} C_X = -3\mathrm{Ca_c}^{2/3} \frac{1 - V_s H}{H^2} \tag{11}$$

$$\alpha\beta\mathrm{Ca_c}^{2/3}(C - C_f) + V_s\tilde{\Gamma} - \tilde{\Gamma}_f = 0 \tag{12}$$

where we introduce the coefficient β defined by $h_f = \beta r_m \mathrm{Ca_c}^{2/3}$ (which is the quantity that we are trying to determine) and the coefficient $\alpha = r_m c_{cmc}/\Gamma_{cmc}$. The coefficient α is a crucial non dimensional parameter of our model, which compares the concentration of surfactants in the bulk to that at the interface. It compares r_m to the length $l_{cmc} = \Gamma_{cmc}/c_{cmc}$, which is the thickness of a liquid layer containing as many surfactants as the corresponding interface, at the cmc. Depending on the surfactants used, it can range from 1 µm to 1 cm, and accordingly α ranges from 1 to 1000 for millimetric menisci.

3.2. Boundary conditions and resolution

For numerical reasons, the boundary conditions must be imposed in the flat film region. As $X \to +\infty$:

$$\begin{aligned} &H = 1, H_X = 0, H_{XX} = 0 \\ &C = C_f \\ &V_s = 1 \end{aligned} \tag{13}$$

The integration is started for $H = 1 + \epsilon_0$ and $X = X_0$ with ϵ_0 a small but finite quantity. The starting values for the other variables and the derivatives

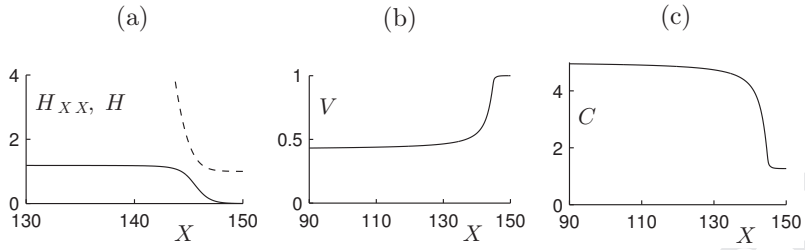

Figure 3: (a): profile $H(X)$ of the dynamical meniscus (dashed line), for $\mathrm{Ca_c} = 10^{-4}$, $\alpha = 60$, $C_m = 5$, $K_\Gamma = 0.001$. We only show a portion of the solution, which is computed from $X = 150$ (flat film) to $X = 0$ (static menisus). The solid line is the curvature of the profile H_{XX}: it reaches a constant value $H_{XX}^{-\infty} \approx 1.19$ towards the static meniscus. (b): a direct illustration of interface stretching is given by the interfacial velocity V_s, which is much lower towards the static meniscus ($V_m \approx 0.42$) than the imposed velocity in the flat film ($V_s(+\infty) = 1$). (c): Marangoni stresses at the interface are related to the distribution of surfactant along the film. In this example, we impose $C(-\infty) = C_m = 5$, and the concentration in the film is much lower ($C_f \approx 1.27$).

of H are found by linearizing the problem in the flat film region. The profile is then integrated to $X = 0$, towards the static meniscus.

Typical profiles are shown in figure 3. The important feature is that we choose X_0 to be large enough that both H_{XX}, V_s and C tend towards well converged constant values as X decreases. This ensures the validity of the asymptotic matching to the static meniscus.

3.3. Matching to the static meniscus

The matching to the meniscus imposes that the curvature tends to $1/r_m$ for negative x. This condition can be written with non dimensional variables as

$$\frac{1}{r_m} = h_{xx}(-\infty) = H_{XX}^{-\infty} \frac{\mathrm{Ca_c}^{2/3}}{h_f} \tag{14}$$

Given $h_f = \beta r_m \mathrm{Ca_c}^{2/3}$ this imposes

$$\beta = H_{XX}^{-\infty} \tag{15}$$

This numerical parameter β appears in equation 12, and it can thus not be freely chosen. Instead, the matching to the meniscus requires to solve the

implicit equation $\beta = H_{XX}^{-\infty}(\beta)$. With β^* the solution of this equation, the film thickness is obtained as:

$$h_f = \beta^* r_m \mathrm{Ca_c}^{2/3} \tag{16}$$

In Frankel's problem, the solution is $h^{Fr} = 1.34 r_m \mathrm{Ca}^{2/3}$ with a capillary number $\mathrm{Ca} = \eta V/\gamma_m$. To compare our predictions to Frankel's, we use the fact that $h_f/h^{Fr} = (\gamma_{cmc}/\gamma_m)^{2/3}\beta^*/1.34$. Note that, as the surface tension variation is very small above the cmc, Ca and $\mathrm{Ca_c}$ differ significantly only below the cmc and the distinction between both is made only when necessary.

Lastly, since the concentration of surfactants is in practice imposed in the static meniscus, a shooting method is used to select the right value of C_f (concentration in the film), given the value of C_m (in the static meniscus) that is imposed.

This procedure allows us to solve the problem, given the following set of independent numerical parameters: C_m, $\mathrm{Ca_c}$, α and the parameters of the equation of state and of the isotherm equation $\tilde{\gamma}(0)$, K_Γ and ξ.

4. Results and discussion

4.1. Influence of the capillary number

Figure 4.a shows the predicted value of h_f/h^{Fr} as a function of Ca (in the range 10^{-6} to 10^{-2}), and for $\alpha = 60$, $\tilde{\gamma}(0) = 2.06$, $K_\Gamma = 0.001$ and $C_m = 5$. Figure 4.b shows the value of the velocity in the static meniscus V_m for the same parameters.

Frankel's prediction, which corresponds to a vanishing interface extension, is recovered within 5 %, for $\mathrm{Ca} < 10^{-5}$. Consistently, as seen on figure 4.b, the velocity difference $1 - V_m$ between the static meniscus and the film, hence interface stretching, is negligible at these low capillary numbers. For some critical capillary numbers interface deformation becomes relevant, as illustrated by the larger velocity difference. Accordingly, h_f departs from Frankel's law.

A higher capillary numbers, there is no direct relation between interface stretching and film thickness, as evidenced by the fact that the non-monotonic

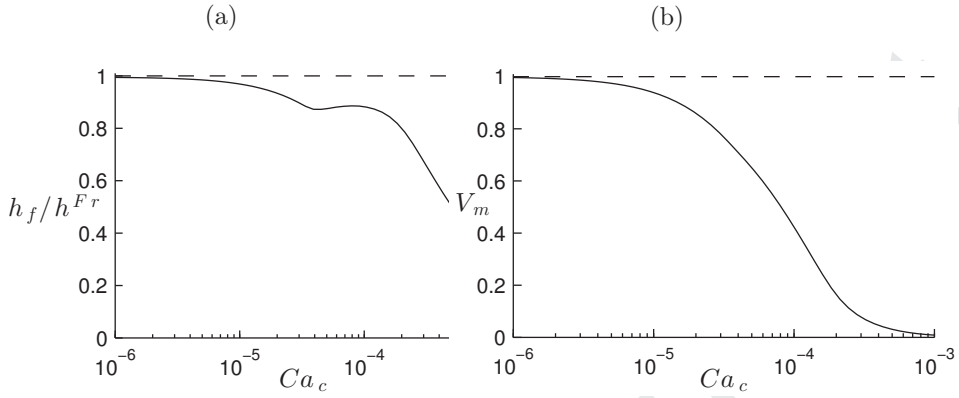

Figure 4: (a): Thickness of the film h_f/h^{Fr} as a function of Ca. (b): Interfacial velocity in the meniscus V_m, as a function of Ca.

behavior of h_f/h^{Fr} for intermediate Ca is not observed for V_m. Note that the physical thickness of the film ($h_f = \beta^* r_m \mathrm{Ca}^{2/3}$) does increase monotonically with Ca.

4.2. Scaling law analysis for the velocity

Although there is no direct relation between the velocity difference δv_s between the film and the static meniscus and the thickness of the film h_f, deviation from Frankel's law only occur for significant interface stretching, that is values of δv_s of order one. A simple law can be derived for this parameter, based on the mass conservation. In this scaling law analysis, we separate formally the dynamic meniscus from the static part and the flat film region, as sketched on figure 5. We limit our analysis to small deviations from Frankel's law. Γ, c, γ and v_s are assumed constant within the film (with respective values Γ_f, c_f, γ_f, U) and in the static meniscus ($\Gamma_m = \Gamma + \delta\Gamma$, $c_m = c + \delta c$, $\gamma_m = \gamma - \delta\gamma$, $v_m = U - \delta v_s$). We focus on the regime of small interfacial stresses, and we treat the problem at first order in δc and δv_s.

At steady state, the net flux of surfactants going through the dynamic meniscus must be zero:

$$(c + \delta c)q + (\Gamma + \delta\Gamma)(U - \delta v_s) = cq + \Gamma_f U$$

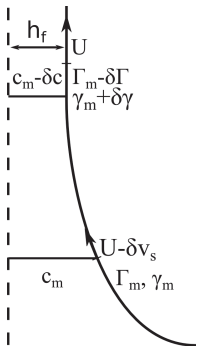

Figure 5: Sketch of half a dynamical meniscus.

At first order, using $q \sim r_m \mathrm{Ca}^{2/3} U$, we get:

$$\delta v_s = \frac{U}{\Gamma} \delta\Gamma \left(1 + r_m \mathrm{Ca}^{2/3} \frac{\partial c}{\partial \Gamma}\right) \tag{17}$$

Lastly, the surface tension difference scales like $\delta\gamma \sim \gamma \mathrm{Ca}^{2/3}$ (see equation 1), so that our final prediction for interface stretching is:

$$\frac{\delta v_s}{U} = \mathrm{Ca}^{2/3} \frac{\gamma}{\Gamma} \frac{\partial \Gamma}{\partial \gamma} \left(1 + \frac{r_m}{\partial \Gamma / \partial c} \mathrm{Ca}^{2/3}\right) \tag{18}$$

The surface dominated case corresponds to $r_m \mathrm{Ca}^{2/3} \partial c / \partial \Gamma \ll 1$. In this limit, the predictions of the elastic interface model are expected and recovered, as verified in the section 4.3.

On the other hand, for a large meniscus radius, or above the cmc where $\partial \Gamma / \partial c$ is very small, surfactants in the bulk are dominant ($r_m \mathrm{Ca}^{2/3} \partial c / \partial \Gamma \gg 1$). A new behavior is observed, which depends on the bulk concentration, as shown in section 4.4.

In non-dimensionnal variables, equation 18 becomes

$$\delta V_s = 1 - V_m = {\mathrm{Ca_c}}^{2/3} (\tilde{\gamma}(0) - 1) \frac{\tilde{\gamma}^{1/3}}{\tilde{\Gamma}_f} \left(1 + \frac{\alpha}{\tilde{\gamma}^{2/3}} \frac{1}{\partial \tilde{\Gamma} / \partial C} {\mathrm{Ca_c}}^{2/3}\right) \tag{19}$$

The variation of $1 - V_m$ with the capillary number is plotted in figure 6. The two power laws are not well separated, but can still be observed.

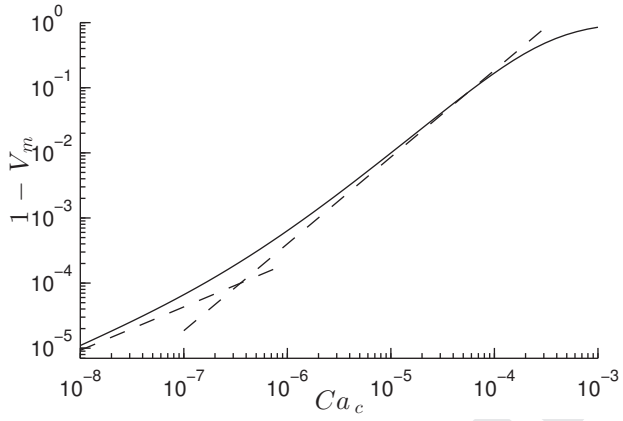

Figure 6: Velocity decrease in the meniscus, as a function of the capillary number Ca, for $C_m = 5$, $\alpha = 1000$ and $K_\Gamma = 0.1$. $\delta V = 1 - V_m$, i.e. interface stretching, increases with Ca. As Ca increases, δV goes from a surface dominated regime, where it increases as $\mathrm{Ca_c}^{2/3}$, to a bulk dominated regime with a $\mathrm{Ca_c}^{4/3}$ dependence, as expected from equation 19 (dashed lines are guides of slope 2/3 and 4/3).

4.3. The limit of elastic interface

If the amount of surfactant in the bulk is much smaller than the amount of surfactant at the interface, then the exchange between interface and bulk becomes negligible and surfactant transport is governed by interfacial convection. In that limit, our model coincides with a model of insoluble surfactant, leading to a purely elastic interface, as studied in [10] and [8]. This limit is recovered when $\Gamma_f \gg ch_f = c_f r_m \beta^* \mathrm{Ca}^{2/3}$, or more precisely (using equation 18) when $\partial\Gamma/\partial c \gg r_m \mathrm{Ca}^{2/3}$. The Ca dependence of the validity criterium simply stresses the fact that the relative contributions of surface and bulk transport vary with Ca, as seen in equation 12.

For simplicity we restrict the comparison to the case $c_m = c_{cmc}$. In that case, the previous condition becomes $\alpha = r_m c_{cmc}/\Gamma_{cmc} \ll \mathrm{Ca}^{-2/3}$ and the Marangoni elasticity is $E = -\Gamma\partial\gamma/\partial\Gamma = \gamma(\tilde{\gamma}(0) - 1)$, as obtained from our equation of state 9.

We compare in figure 7 the results obtained with the elastic model discussed in [10] and the results obtained with our calculations in different regimes. We

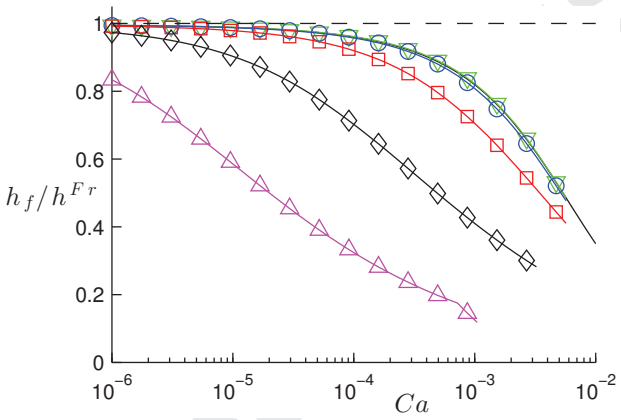

Figure 7: Thickness of the film h_f/h^{Fr} as a function of Ca ($C_m = 1$, so Ca = $\mathrm{Ca_c}$). Symbols are for the present model with $\alpha = 0.01\mathrm{Ca}^{-2/3}$ ($\triangledown$), $\alpha = 0.1\mathrm{Ca}^{-2/3}$ ($\circ$), $\alpha = \mathrm{Ca}^{-2/3}$ ($\square$), $\alpha = 10\mathrm{Ca}^{-2/3}$ ($\diamond$), $\alpha = 100\mathrm{Ca}^{-2/3}$($\triangle$). The other parameters of the calculations are chosen to allow for an easy direct visual comparison with the elastic case and thus test the robustness of the model, and may thus not correspond to real experimental values: $K_\Gamma = 1$, $\tilde{\gamma}(0) = 1.1$. The solid line is the prediction of the model with elastic interfaces, with an elasticity $E/\gamma = 0.1 = \tilde{\gamma}(0) - 1$ [10]. It follows Frankel's law (dashed line) for Ca $< 10^{-4}$, then decreases with Ca.

plot the film thickness, renormalized by Frankel's thickness, as a function of the capillary number. The solid black curve is obtained with the elastic model, with $E/\gamma = 0.1$. For each other curve, obtained with the full model, we set $\tilde{\gamma}(0)-1 = 0.1$, $C_f = 1$ and $\alpha = k\mathrm{Ca}^{-2/3}$, with k a constant. For $\alpha = 0.01\mathrm{Ca}^{-2/3}$ or $\alpha = 0.1\mathrm{Ca}^{-2/3}$, both predictions for the thickness of the film agree, as expected. Frankel's law is observed at small capillary numbers and a thinner film is obtained if $E/\gamma \gg Ca^{2/3}$.

For higher values of α ($\alpha = \mathrm{Ca}^{-2/3}$, $\alpha = 10\mathrm{Ca}^{-2/3}$ or $\alpha = 100\mathrm{Ca}^{-2/3}$), the solubility of the surfactant is increased and the bulk concentration becomes non-negligible with respect to surface concentration. Surface extension can be cured by a reabsorption of surfactants. The surface tension variation for a given interfacial extension is thus reduced at high solubility, which corresponds qualitatively to a smaller effective elasticity. Consistently, the departure from Frankel's law occurs at lower capillary number for larger values of the solubility. Note that, in figure 7, the bulk concentration is fixed: the variation of the ratio c/Γ thus corresponds to a variation of Γ, at constant c, that can be achieved by changing the surfactant used. The influence of the bulk concentration, for a given surfactant, is discussed below.

4.4. Effect of initial surfactant concentration c_m

An important aspect of our model is the ability to predict film thickness variations as a function of the concentration in the meniscus. The most important feature is a strong film thinning observed when the concentration goes from one cmc to several cmc.

The variation of h_f/h^{Fr} with $C_m = c_m/c_{cmc}$ is shown in figure 8, where we plot the result of our calculations for a constant pulling velocity, constant surfactant physicochemical properties, constant meniscus radius and increasing values of bulk concentration. For $1 < C_m < 6$, an important thickness decrease is obtained. Note that Frankel's film thickness $h^{fr} = 1.34(\eta U/\gamma)^{2/3}$, used as a thickness reference, varies slightly with C_m, as the surface tension varies (see the surface tension in the film and in the meniscus in figure 9.b). However, this

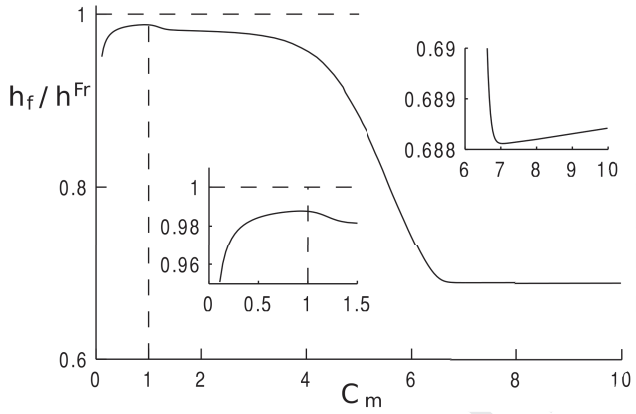

Figure 8: Thickness of the film, rescaled by h^{Fr}, as a function of the imposed concentration of surfactant in the meniscus $C_m = c_m/c_{cmc}$, for $\mathrm{Ca_c} = 10^{-4}$ (i.e. for a constant pulling velocity), $\alpha = r_m c_{cmc}/\Gamma_{cmc} = 60$ and $K_\Gamma = 0.001$. h_f/h^{Fr} increases slowly with C_m for $C_m < 1$, and for $C_m > 6$ (see the zooms on the relevant regions in insets). Between these values, it decreases much more rapidly with C_m. For these values of the parameters, h_f/h^{Fr} always remains significantly smaller than 1.

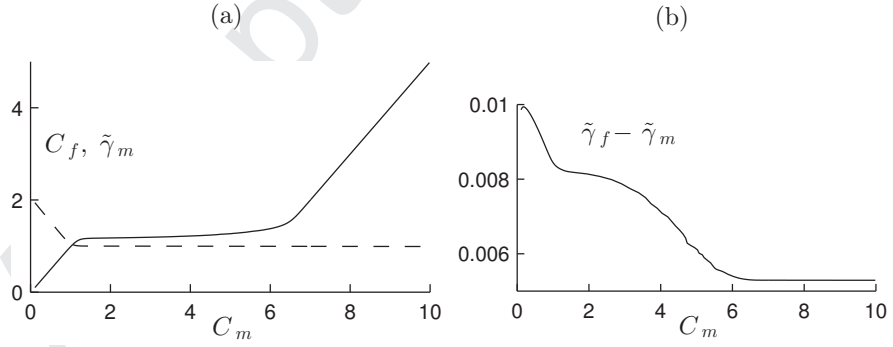

Figure 9: (a): for the same data as figure 8, the concentration in the film $C_f = c_f/c_{cmc}$ (solid line) increases monotonously with C_m. It does, however, also feature three well distinct regimes of very different slopes. Dashed line is $\tilde{\gamma}_m$. (b): for the same data, the surface tension difference $\tilde{\gamma}_f - \tilde{\gamma}_m$ remains very small (below 1 %).

effect is only sensible much below the cmc and does not play any relevant role here.

The observed transition between a film close to the Frankel's film and a much thinner film can be understood on the basis of the velocity scaling given by equation 19. The concentration decreases from the static meniscus to the film, and for $1 < C_m < 6$, the film is almost at the cmc, as seen in figure 9.a. For lower concentrations, the film is entirely below the cmc, whereas for higher concentrations, it is always above the cmc. It means that the non linearity of the isotherm (i.e., the fact that the concentration crosses the cmc, where $\partial\tilde{\Gamma}/\partial C$ changes abruptly) has to be taken into account in the intermediate concentration regime only.

With the parameters of figure 8, we have $K_\Gamma = 10^{-3} \ll \alpha \mathrm{Ca_c}^{2/3} = 0.13 \ll 1$. The second term in equation 19, associated to bulk concentration effects, is thus negligible below the cmc, but non negligible above, as the coefficient $\partial\tilde{\Gamma}/\partial C$ suddenly decreases from 1 to K_Γ. The velocity difference thus jumps from a small value below the cmc to a much higher value above the cmc, thus explaining the sudden thickness decrease for meniscus concentrations slightly above the cmc.

Let us simplify the problem one final time by considering the limit where the surface tension variation above the cmc is negligible and the tension variation below the cmc very large (which corresponds to incompressible interfaces, as in Frankel's work). Starting from a concentration in the static meniscus $C_m > 1$, the concentration must first decrease to the cmc, which generates no interfacial stresses, but does stretches the interface. Below the cmc, the necessary stresses may now be created with negligible concentration difference, hence negligible interface deformation. In other words, the entire interfacial elongation happens above the cmc, and corresponds to a decrease in concentrations from $C_m > 1$ to 1. Interface stretching thus increases with C_m, which results in the thickness decreasing. The real curve is smoothened out by the small surface tension variation above the cmc, and by the finite size of the transition region between the affine regimes of the isotherm. The physical origin of the thickness decrease

still holds: it is a signature of the non linear isotherm.

As visible on the two enlargements of figure 8, the rescaled thickness increases slightly with C_m for $C_m < 1$ and for $C_m > 6$: surprisingly, for a given pulling velocity, the film thickness thus varies in a non-monotonic way with the concentration. For $C_m < 1$ or $C_m > 6$, the film is either always below the cmc or always above, as shown in figure 8. The variation of the surface concentration with the bulk concentration is thus affine: $\partial\tilde{\Gamma}/\partial C$ is either 1 (below the cmc) or K_Γ (above the cmc). Equation 19 can then be simplified into

$$\delta V_s = 1 - V_m = {\mathrm{Ca_c}}^{2/3}(\tilde{\gamma}(0) - 1)\frac{\tilde{\gamma}^{1/3}}{\tilde{\Gamma}}\left(1 + \frac{\alpha}{\tilde{\gamma}^{2/3}}\frac{1}{K_\Gamma}{\mathrm{Ca_c}}^{2/3}\right) \qquad (20)$$

for the case $C_m > 1$ (the case $C_m < 1$ is obtained by setting $K_\Gamma = 1$). In figure 8, $\mathrm{Ca_c}$ (i.e. the pulling velocity) is maintained constant, as well as the physicochemical properties $\tilde{\gamma}(0)$ and α. In the previous equation, only $\tilde{\gamma}$ and $\tilde{\Gamma}$ vary with the concentration in the meniscus, and the main effect is the affine increase of $\tilde{\Gamma}$ with C_m. Consequently, the velocity variation along the film decreases with C_m, and the film thickness increases.

4.5. Comparison with experiments

As a final summary of our results, we compare our model to experimental data published by Saulnier and collaborators [8]. One of the central results of their work is the fact that deviation from Frankel law is observed above a certain capillary number, for a solution of $C_{12}E_6$ surfactant. Most importantly, they measured film thicknesses for different surfactant concentrations (C_m = 1, 3, 5 and 10 in our notations), and showed that this transition capillary number decreases with C_m.

As we mentioned in the previous section, our model does reproduce qualitatively this behavior. More precisely, we show on figure 10.a the best fit of their data by our model, with $K_\Gamma = 0.0012$ as the only adjustable parameter ($\alpha = 63$ has been estimated from $\Gamma_{cmc} = 3\,10^{-6}$ mol/m^2 and $c_{cmc} = 7.3\,10^{-5}$ mol/L, as measured in [18]). In our model, $\mathrm{Ca_c}$ is imposed, instead of Ca, however, the

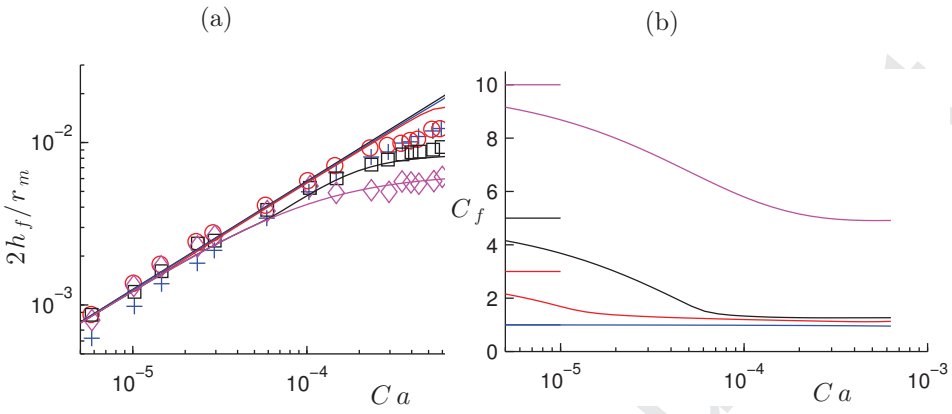

Figure 10: (a): experimental film thicknesses measured by Saulnier and coworkers[8] for a solution of $C_{12}E_6$ at the cmc (+), at 3 cmc (○), at 5 cmc (□) and at 10 cmc (◇). Solid lines are predictions of our model with the corresponding value of C_m, $\alpha = 63$ (computed from experimental values of Γ_{cmc} and c_{cmc}), $\tilde{\gamma}(0) = 2.1$ (computed from the measured value of γ_{cmc}) and $K_\Gamma = 0.0012$ (fitted). (b): our model also predicts the surfactant concentration C_f in the film. Short horizontal lines show the concentration that is imposed in the meniscus.

difference between the two parameters is negligible above the cmc, as γ remains very close to γ_{cmc}.

Our model captures the Ca and C_m dependance of the thickness quite well, except for the smaller C_m where it underestimates deviations from Frankel's law.

The relevance of the fitted value of K_Γ is difficult to evaluate, since most studies on surface tension focus on concentrations below the cmc, and measuring γ with the appropriate precision is not straightforward. In one study [18], Stubenrauch and collaborators measured the surface tension well above the cmc. By fitting their data, we found a value of K_Γ on the order of 0.01.

Our model also predicts the surfactant concentration C_f in the extracted film (figure 10.b). As Ca increases, the stresses needed to extract the film increase, hence C_f decreases to generate a larger surface tension difference across the system. For $C_m = 3$ and $C_m = 1$, the concentration C in the dynamical meniscus becomes low enough that it reaches the transition region of our isotherm (with $\xi = 0.15$, the transition region starts at $C \approx 1.3$) for Ca $> 10^{-4}$.

The prediction is thus sensitive, for these C_m, to the exact function used to describe this region. This may explain the discrepancy between our model and the data.

Lastly, our computations predict values of C_f significantly different from C_m (by up to 50 %). We believe that measuring this quantity would provide the most direct way to confirm or infirm the relevance of our work to experimental situations.

5. Conclusion

In the present study, we predict the steady state thickness of soap films pulled from a bath of surfactants at constant speed. The originality of our work lies in the fact that we do not assume a particular effective interfacial rheology (i.e., incompressible or elastic or viscous interface). Instead, we take explicitly into account the transport of surfactant molecules, and we deduce the Marangoni stresses at the interface, which serve as boundary condition for the hydrodynamics within the film, from their repartition.

In our model, the apparent rigidification of the interfaces comes explicitly from depletion/confinement effects: interface stretching lowers locally the concentration of surfactants, because molecules in the bulk adsorb on the newly created interface. The peculiar thinness of the films make this mechanism particularly efficient to create interfacial stresses. We use two key approximations to track surfactants: their concentration is supposed homogeneous within the thickness of the film, and bulk and surface adsorbed surfactants are supposed at equilibrium.

We show that this mechanism suffices to create the necessary stresses to pull a film out of a reservoir. For low enough capillary numbers, Frankel's law is recovered. Much like what is observed in experiments, deviations from this law occur at higher pulling velocities. We identify a regime of "insoluble" surfactants, where the elastic interface model is recovered. Outside of this regime, bulk molecules have to be taken into account and lead to a less "rigid" interfaces.

Most importantly, with our approximations, the entire problem is computed from equilibrium properties of the surfactant molecules. In particular, the resulting Marangoni stresses, hence the thickness of the film, depend strongly on the form of the adsorption isotherm and the equation of state. We use here a simplified form for these two functions, but more realistic ones could be as easily incorporated. In fact, we found that the non linearity of the adsorption isotherm (namely the fact that its slope change abruptly around the cmc) is crucial to the generation of films.

Lastly, the most obvious prediction of our model is the thickness of the film, because it can be easily measured. We show that its results are compatible with available data by Saulnier and coworkers [8]. Our calculations additionally compute the repartition of surfactants, and the interfacial velocity. Although these quantities are much harder to measure in experiments, they are much more closely related to the mechanisms at work: the lower concentration in the film is a direct effect of depletion, while the lower interfacial velocity in the static meniscus comes from interface stretching.

Ackowledgements

We would like to thank E. Rio and B. Dollet for fruitful discussions. J. S. acknowledges financial support from Région Bretagne (CREATE MOUSPORE) and Agence Nationale de la Recherche (ANR-13-PDOC-0014-01-HYDROSURFDYN).

References

[1] L. Landau, B. Levich, Dragging of a liquid by a moving plate, Acta Physicochim. USSR 17 (1942) 42.

[2] B. V. Derjaguin, Thickness of liquid layer adhering to walls of vessels on their emptying, Acta physicochim URSS 20 (1943) 349.

[3] K. J. Mysels, K. Shinoda, S. Frankel, Soap films: Study of their thinning and a bibliography, Pergamon, New-York, 1959.

[4] R. Krechetnikov, G. M. Homsy, Surfactant effects in the Landau Levich problem, J. Fluid Mech. 559 (2006) 429–450.

[5] O. O. Ramdane, D. Quéré, Thickening factor in Marangoni coating, Langmuir 13 (11) (1997) 2911–2916.

[6] A. Q. Shen, B. Gleason, G. H. McKinley, H. A. Stone, Fiber coating with surfactant solutions, Phys. Fluids 14 (2002) 4055.

[7] J. Lal, J.-M. di Meglio, Formation of soap films from insoluble surfactants, J. Colloid Interface Sci. 164 (2) (1994) 506–509. doi:10.1006/jcis.1994.1196.

[8] L. Saulnier, F. Restagno, J. Delacotte, D. Langevin, E. Rio, What is the mechanism of soap film entrainment?, Langmuir 27 (22) (2011) 13406–13409. doi:10.1021/la202233f.

[9] L. Champougny, B. Scheid, F. Restagno, E. Rio, The role of surface elasticity in liquid film formation: unifying Frankel and Landau-Levich-Derjaguin configurations, arXiv preprint (14024640).

[10] J. Seiwert, B. Dollet, I. Cantat, Theoretical study of the generation of soap films: role of interfacial visco-elasticity, J. Fluid Mech. 739 (2014) 124–142.

[11] Y. Couder, J.-M. Chomaz, M. Rabaud, On the hydrodynamics of soap films, Physica D 37 (1989) 384–405.

[12] M. van den Tempel, J. Lucassen, E. H. Lucassen-Reynders, Application of surface thermodynamics to Gibbs elasticity, J. Phys. Chem. 69 (1965) 1798–1804.

[13] D. Quéré, A. de Ryck, Le mouillage dynamique des fibres, Ann. Phys. 23 (1998) 1–151.

[14] I. Cantat, Liquid meniscus friction on a wet wall: bubbles, lamellae and foams, Phys. Fluid. 25 (2013) 031303.

[15] C.-H. Chang, E. I. Franses, Adsorption dynamics of surfactants at the air/water interface : a critical review of mathematical models, data, and mechanism, Colloids Surf. A 100 (1995) 1–45.

[16] P. G. de Gennes, Young soap films, Langmuir 17 (8) (2001) 2416–2419. doi:10.1021/la0015381.

[17] M. Durand, D. Langevin, Physicochemical approach to the theory of foam drainage, Eur. Phys. J. E 7 (2002) 35.

[18] C. Stubenrauch, O. J. Rojas, J. Schlarmann, P. M. Claesson, Interactions between nonpolar surfaces coated with the nonionic surfactant hexaoxyethylene dodecyl ether C12E6 and the origin of surface charges at the air/water interface, Langmuir 20 (2004) 4977–4988.